Journal of Sound and Vibration 348 (2015) 224–238

Contents lists available at ScienceDirect

Journal of Sound and Vibration

journal homepage: www.elsevier.com/locate/jsvi

Identification of backbone curves of nonlinear systems from resonance decay responses

Julián M. Londoño [a,*], Simon A. Neild [a], Jonathan E. Cooper [b]

[a] Department of Mechanical Engineering, University of Bristol, Queens Building, University Walk, Bristol BS8 1TR, UK
[b] Department of Aerospace Engineering, University of Bristol, Queens Building, University Walk, Bristol BS8 1TR, UK

ARTICLE INFO

Article history:
Received 13 August 2014
Received in revised form
24 February 2015
Accepted 5 March 2015
Handling Editor: L.N. Virgin
Available online 26 March 2015

ABSTRACT

Backbone curves can offer valuable insight into the behaviour of nonlinear systems along with significant information about any coupling between the underlying linear modes in their response. This paper presents a technique for the extraction of backbone curves of lightly damped nonlinear systems that is well suited for the experimental investigation of structures exhibiting nonlinear behaviour. The approach is based on estimations of the instantaneous frequency and the envelope amplitude of a decaying response following a tuned steady-state oscillation of the system. Results obtained from simulations and experiments demonstrate that the proposed procedure is capable of achieving an accurate estimation of the backbone curves and damping ratios of the system provided that the premise of damping having low impact on its oscillation frequency is met.

1. Introduction

There has been much recent interest in predicting the behaviour of structures containing nonlinearities. This is, in part, the result of the latest developments in new materials together with the increasing computational capabilities that have brought to light a variety of novel design solutions to diverse engineering problems. For instance, a number of innovative structures, such as the civil aircraft A380 XWB and 787 Dreamliner, are notably more efficient and lightweight. Such systems have less inherent damping and are particularly flexible and therefore more susceptible to nonlinear effects. Consequently, the understanding of nonlinear dynamic systems and their performance in operational and under extreme loading conditions is an increasingly important research topic with potentially strong impact in many industrial sectors.

The presence of nonlinearities can be detected via standard techniques in experimental testing [1,2]. For instance, the variation of conventional Frequency Response Functions (FRF) obtained for different constant excitation levels, and also differences in the reciprocity between pairs of driving point FRFs, can be judged as clear evidence of nonlinear behaviour. However, the localisation, characterisation and quantification of such nonlinear behaviour are still open research topics [3]. A tool capable of offering a better understanding of the behaviour of nonlinear systems is the backbone curve [2,4] which defines the natural frequency as a function of the amplitude of the system response when neither damping nor forcing are present. The backbone curves provide a valuable description of the system dynamics that may allow for characterising and quantifying active nonlinearities whilst highlighting the interactions that may occur within the system, enabling for instance, the study of modal energy exchange due to nonlinearities, that cannot be analysed by conventional linearised

* Corresponding author.
E-mail addresses: Julian.Londono@bristol.ac.uk (J.M. Londoño), Simon.Neild@bristol.ac.uk (S.A. Neild), J.E.Cooper@bristol.ac.uk (J.E. Cooper).

http://dx.doi.org/10.1016/j.jsv.2015.03.015
0022-460X/

methods. In addition, it opens up the possibility of using backbone curves to identify or update nonlinear characteristics within a model based on the experimental response [5,6].

A technique for extracting backbone curves consists in the estimation of both the instantaneous amplitude and frequency along a free vibration response of the nonlinear system. In this context, a key approach is based on the application of the Hilbert transform to free vibration data, see for example the significant contribution made by Feldman [7]. Therein, a set of equations are proposed to estimate instantaneous characteristics such as amplitude, frequency and damping. Feldman extended and improved the method in [8], where the identification of nonlinear elastic forces acting in asymmetric systems was studied, leading to an effective identification. However, as discussed later, high-frequency superharmonics components of the Hilbert transform can be very sensitive to noise and so be detrimental to its estimation capabilities. Another approach is based on the use of Wavelets transform; in [9], a method for the identification of damping in MDOF systems was proposed by examining the system impulse response decomposed into the wavelets' time-scale domain. The method was further developed to extract ridges and skeletons of the Wavelets transform using optimisation algorithms based on simulated annealing [10]. These features were then employed to obtain the system backbone curve with a view to identify the linear and nonlinear parameters.

It is of interest to investigate structures that are at a first approximation linear at low vibration levels, but contain active nonlinear elements which become significant at larger excitation levels; typical of many industrial type structures. The interest here is to study the free vibration response originated from initial conditions that lie on a particular steady-state response of the nonlinear system. The Resonance Decay Method (RDM) [11] may be used, as this enables the excitation of modes of the system independently. Once the structure is vibrating at the desired resonance condition, the forcing is removed and the resulting free vibration response analysed. This strategy has proven to be able to isolate distinctive characteristics of several nonlinear systems through the case of fitting system parameters to the transient response [12–14].

In this paper, the RDM method is modified to estimate backbone curves for nonlinear systems. A procedure for the estimation of instantaneous amplitude, frequency and damping from decaying responses originated from steady-state oscillations is proposed. The approach enables measurements to be made in regimes of large displacements, where nonlinearities are more active. This facilitates more information to be deduced from the backbone curves, thus potentially enabling a realistic identification of the nature of nonlinearities. The approach is validated using a number of simulated systems with nonlinearities typically encountered in common engineering applications. Additional results are also included to show the applicability of the procedure on real experiment data.

This paper is organised as follows. Section 2 introduces the procedure proposed in this work. Simulated single-degree-of-freedom (SDOF) systems with nonlinear elements are used in Section 3 to show how backbone curves are estimated. The procedure is then validated using experimental data in Section 4. The following section presents the extension of this procedure to multi-degree-of-freedom (MDOF) systems, finishing with the final comments and remarks in the conclusions.

2. Estimation of backbone curves

In this section a method for measuring the backbone curves from appropriate structural responses and then for extracting frequency and damping information are discussed.

2.1. Obtaining the decay response

Transient responses contain information about all of the underlying fundamental features of dynamical systems, including those properties that are susceptible to change as a function of the oscillation amplitude. In particular, the interest is to examine free vibration records originated when setting the system free after obtaining a desired resonant response under harmonic forcing.

Consequently, in this procedure the signal used to extract the backbone curves of the nonlinear system is generated in accordance with the Resonance Decay Method (RDM) [11]. In this technique, individual modes of the system can be excited independently by applying an appropriated force pattern previously estimated. Such a force pattern is determined by using the normal-force mode appropriation method, that enables for extracting the undamped natural frequency and normal-modes shapes of a structural system [15]. After the appropriated force pattern is computed, this is applied to the system at the relevant frequency using harmonic excitation. When the structure is responding at the desired resonance condition, the input is removed and the model undergoes free vibration from the resonant response. As long as the level of vibration in the steady state is large enough to activate the structural nonlinearities, the generated decaying response offers significant information about the system and related parameters.

Once the decay response of the system is obtained, two main features, namely instantaneous frequency and amplitude envelope, can be estimated in the interest of extracting the backbone curves of the system.

2.2. Instantaneous frequency assessment

Whilst there are many procedures for calculating instantaneous frequency, such as the Wigner–Ville distribution (WVD) [16] and the Hilbert transform (HT) [7], the process presented here is based on the detection of the zero-crossing points of the response signal and the use of a standard interpolation algorithm to determine the crossing times. Noisy signals are firstly smoothed out around the crossing points using a suitable moving average filter. This combined process reduces errors in the frequency assessment due to both the unlikely event of having sampled points coinciding with zero-passing times, and the undesirable consequence of having false crossing events caused by the presence of noise. We found that this procedure provides a better frequency estimation particularly towards either ends of the decay record, where procedures such as WVD and HT lead to greater uncertainty as their estimation are based on fewer non-zero points at both signal ends. In addition, HT seems to be much more sensitive to noisy data, this could be explained as it requires the derivative of the real and the imaginary part of the transformation to estimate the instantaneous frequency (see also Section 3.1).

Once the sequence of the crossing times (t^o) is determined, the first estimation of the instantaneous frequency at the i-th crossing point $\hat{f}(t_i^o)$ can be computed such that

$$\hat{f}(t_i^o) = \left(t_{i+1}^o - t_{i-1}^o\right)^{-1} \tag{1}$$

Note that the frequency is estimated from the inverse of the instantaneous period along one complete cycle and assigned to the crossing time at the center of it.

One further process is needed to smooth out imperfect predictions of Eq. (1). The final estimator delivers only the dominant frequency variation in the decaying signal. A moving average (MA) filter is proposed to shape the final instantaneous frequency estimation. In spite of its simplicity, the moving average filter offers optimal properties in reducing random noise while is able to retain a sharper step response. A N-th order MA filter is defined as

$$f(t_i^o) = \frac{1}{N}\sum_{j=0}^{N-1} \hat{f}\left(t_{i+j}^o\right) \tag{2}$$

and the filter order needs to be selected on a case-by-case basis in accordance with the level of noise present in the signal.

It is worth noting that a backbone curve corresponds to the solution of the nonlinear system on the hypothesis that both forcing and damping are null, or equivalently, that the forcing compensates the damping forces in the system at those particular frequencies and amplitudes. In line with this, the procedure described above assumes that the instantaneous frequency estimated is not rapidly altered by the dissipative forces acting on the system.

2.3. Instantaneous amplitude

A simple strategy for estimating the instantaneous amplitude over the decay response is to extract the response envelope by tracking the peaks of the signal within each individual zero-crossing time interval.

In the proposed procedure, the maximum absolute value of the signal X and its corresponding occurring time (t_i^a) are retrieved within each interval $\{t_i^o, t_{i+1}^o\}$ using the equations

$$\hat{a}_i = \max_{\forall t | \{t_i^o \geq t \geq t_{i+1}^o\}} |X(t)| \tag{3}$$

$$t_i^a = t \overset{\text{iff}}{\Leftrightarrow} \hat{a}_i = |X(t)| \tag{4}$$

Now, define $\mathcal{I}(t)$ as a polynomial interpolating function of the sequence of numbers $[\hat{a}_i, t_i^a]$ that defines the envelope of the decaying time signal. The results presented in this paper correspond to a first-order polynomial interpolator. The instantaneous amplitude is estimated from the interpolating function at the same time at which the instantaneous frequency has been evaluated, thus

$$A(t_i^o) = \mathcal{I}(t)_{\forall t = t_i^o} \tag{5}$$

Subsequently, the backbone curve can be obtained as a function of frequency and amplitude parametrised by the time, since the forcing has been removed. Thus, it is enough to pair the sequences $A(t_i^o)$ and $f(t_i^o)$ correspondingly.

2.4. Effective damping ratio

The dissipative characteristics of the system can be assessed by examining the envelope of the decaying response. For a classical SDOF system represented by the well-known equation

$$\ddot{x} + 2\xi\omega_n\dot{x} + \omega_n^2 x = 0 \tag{6}$$

and the envelope of the free vibration response can be written in terms of the system parameters and the initial condition as

$$A(t) = A_0 e^{-\xi\omega_n t} \tag{7}$$

Note that the damping action is accounted for by the exponential term. This expression can be generalised to allow for the instantaneous frequency and damping to change, as would occur in a nonlinear system, by rewriting Eq. (7) as

$$A(t) = A_0 e^{-\xi(t)\omega_0(t)t} \tag{8}$$

From this, the effective damping can be computed as

$$\xi(t_i^o) = \frac{1}{\omega_0(t_i^o)t_i^o}\left(\ln(A_0) - \ln\left(A(t_i^o)\right)\right) \tag{9}$$

where $\omega_0(t_i^o) = 2\pi f(t_i^o)$ represents the instantaneous angular frequency in rad/s. Thus, the effective damping ratio ξ can be estimated from the tangent slope of the envelope of the decaying response plotted in semi-logarithmic scale with respect to time.

As will be shown later, in the case of MDOF systems, the structural response can be expressed in terms of the linear modal coordinates. Then, the approach presented above can be applied to each modal response individually to allow for the estimations of backbone curves in modal space. Note that in doing so, it is assumed that the envelope of each mode is described by a time-variable exponentially decaying function.

3. Application to nonlinear SDOF systems

In this section a series of nonlinear SDOF systems are used to illustrate the applicability of the procedure presented above. The aim is to show the validity of this approach in estimating backbone curves of nonlinear systems, along with its differences with respect to existing methods. The nonlinear systems examined here are modelled as

$$m\ddot{x} + c\dot{x} + kx + f_c(\dot{x}) + f_k(x) = F \tag{10}$$

where $f_c(x)$ and $f_k(x)$ represent generic nonlinear damping and nonlinear restoring force respectively. A number of nonlinearities typically encountered in common engineering applications are examined. Table 1 summarises the type of nonlinearities and the numerical values used in each case. In addition, the parameters of the underlying linear system named mass, damping coefficient and stiffness are assumed to be $m = 1.5$ kg; $c = 0.8$ N s/m and $k = 6000$ N/m respectively. These values have been taken from [17] to allow for a direct comparison with the method presented therein.

In order to validate the results, analytical expressions for the stiffness and damping functions have been derived using the Harmonic Balance method to solve the nonlinear differential equations [2, p. 81]. Table 2 presents the true or *nominal* nonlinear stiffness and damping for each case as well as the corresponding approximations, the so-called *effective* stiffness and damping for the system in Eq. (10). Here, the first-order expansion of the Harmonic Balance approximation has been considered, i.e., the effective expressions correspond to the stiffness and damping of a linearised system under the assumption that, in the steady state, this responds at the same frequency as the harmonic excitation $F = F_0 \sin(\omega_f t)$.

Hence the backbone curve and damping skeleton estimated by applying the procedure presented above are further processed to approximate (i) the effective stiffness by multiplying the square of the estimated instantaneous angular frequency by the structural mass m; and (ii) the effective damping using $c_{\text{eff}} = 2m\xi(t_i^o)\omega_0(t_i^o)$. These approximations will be then compared against their analytical predictions in Table 2. A numerical integrator based on Runge–Kutta methods (Matlab ODE45) was used to solve the nonlinear differential equation of motion under different loading conditions for each of the aforementioned set of nonlinear parameters. An integration step of 0.001 s was used in all of the simulations.

Case 1: *Cubic stiffness*. The initial step is to generate the decaying response required to extract the skeleton curves of the system. For the case of SDOF systems there is no need to start the decay from a steady-state harmonic oscillation as explained in Section 2.1, since only one main resonance frequency is involved in the response. Therefore any initial displacement (or velocity) large enough to activate the nonlinearity is adequate.

Table 1
Nonlinearities considered in the example SDOF systems.

System's nonlinearity	$f_c(\dot{x})$ (N)	$f_k(x)$ (N)
Cubic stiffness	0	$7 \times 10^6 x^3$
Quadratic damping + cubic stiffness	$8\,\dot{x}\lvert\dot{x}\rvert$	$7 \times 10^6 x^3$
Dry friction	$0.85\ \text{sign}\,(\dot{x})$	0

Table 2
Analytical expressions of the nominal (true) and effective (first-order approx.) stiffness and damping for the system in Eq. (10) with the nonlinearities in Table 1.

	Cubic stiffness	Quadratic damping	Dry friction damping
Nominal	k_{nx}^3	$c_1\dot{x}\lvert\dot{x}\rvert$	$c_2\text{sign}\,(\dot{x})$
Effective	$k + \frac{3}{4}k_n x^2$	$c + \frac{8}{3}\frac{c_1\omega_n x}{\pi}$	$c + 4\frac{c_2}{\pi\omega_n x}$

Fig. 1 presents the results of applying the procedure presented above on the decaying response of the SDOF system with cubic stiffness from the initial condition $[4\times10^{-3}\ \mathrm{m}, 0\ \mathrm{m/s}]$. The left-hand panels illustrate how amplitude, instantaneous frequency and damping are tracked along the decay using the procedures discussed in Section 2. Similarly, the right-hand panels show the final results: the estimated backbone curve and damping ratio skeleton. A sharp estimation of the backbone curve is achieved. The estimation of the damping ratio is more sensitive to the fidelity of the response data, particularly at smaller amplitudes where inaccurate measurements are more likely to occur. Nevertheless, a clear trend of the damping ratio can still be easily identified, allowing for applying subsequent curve-fitting approaches if required.

The estimated effective stiffness and damping are shown in Fig. 2 as continuous line. The corresponding analytical approximations are plotted using dashed lines for comparison. Note that the identified effective stiffness closely follows the theoretical prediction which implies that the estimation of both the instantaneous frequency and amplitude, that together define the backbone curve, has been accomplished successfully. In spite of minor differences at larger amplitudes, the effective damping coefficient satisfactorily matches its theoretical counterpart. As discussed later in *Case* 3, these minor differences stem from the noncompliance with the assumption of damping having no influence on the system's vibration frequency.

Case 2: *Quadratic damping and cubic stiffness*. The second case corresponds to a SDOF system with a combination of quadratic damping and cubic stiffness. As before, only the decay record from an initial condition large enough to activate the combined nonlinearities is required. The initial condition used in this example is $[5\times10^{-3}\ \mathrm{m}, 0\ \mathrm{m/s}]$.

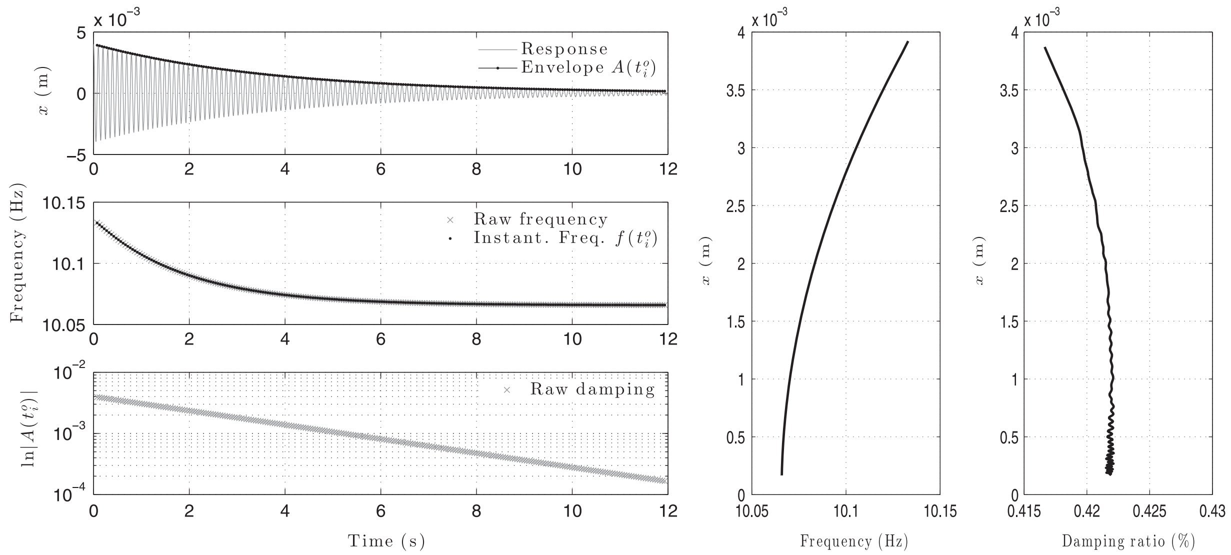

Fig. 1. SDOF with cubic stiffness. (Left) Estimation of envelope, instantaneous frequency and damping. (Right) Backbone curve and damping skeleton.

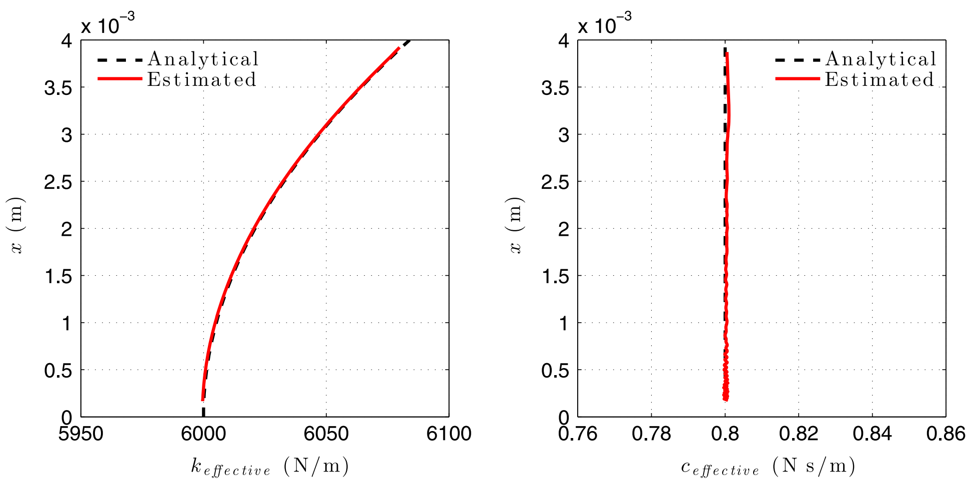

Fig. 2. Effective stiffness and damping estimated from the backbone curve of the SDOF with cubic stiffness.

Fig. 3 presents the results in terms of the estimated effective stiffness and effective damping. Again the corresponding analytical approximations are plotted in dashed lines. These results show good agreement between the estimated and the analytical parameters. Even though the processed decay response is affected by the two nonlinearities blended together, the procedure is able to distinguish their influence and produce a clear estimation of both the damping and stiffness behaviour.

Case 3: *Dry friction*. The case of a SDOF oscillator with dry friction is now investigated. To estimate the backbone curve, the required decaying response record is generated from the initial condition [0.2 m, 0 m/s]. Again an accurate prediction of the nonlinear characteristic is achieved implying a successful estimation of the backbone curve. Interestingly, small differences can be seen in the left panel in Fig. 4 when comparing the predicted effective stiffness at small values of amplitude. Note that as the amplitude of oscillation reduces, the dry friction produces damping forces that are increasingly more significant in the system response. This balance of forces affects the observed instantaneous frequency. The procedure proposed here assumes that the instantaneous frequency is not significantly affected by damping, which is not the case within low vibration amplitude regime.

3.1. Differences with existing methods

In the literature, several methods offer the possibility of approximating backbone curves. For the sake of completeness, two established strategies well suited to extract backbone curves of nonlinear systems are considered in this section to further validate the proposed procedure as well as to highlight some differences.

Firstly, the approach presented by Feldman in [7,8] that uses the Hilbert transform to estimate both envelope and instantaneous frequency is explored. Fig. 5 presents the results of estimating the amplitude envelope and instantaneous frequency from decay records that correspond to the example of a SDOF with a cubic stiffness. Note that the frequency was

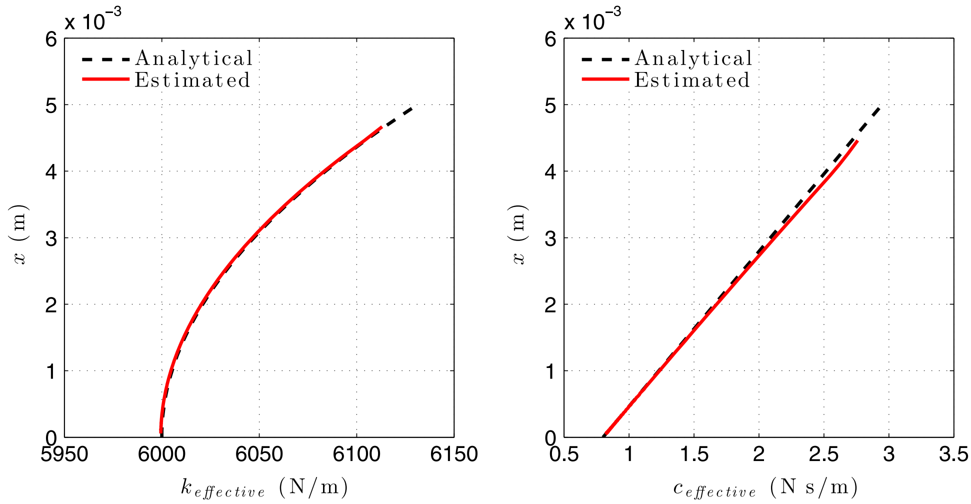

Fig. 3. Effective stiffness and damping estimated from the backbone curve of the SDOF with quadratic damping and cubic stiffness.

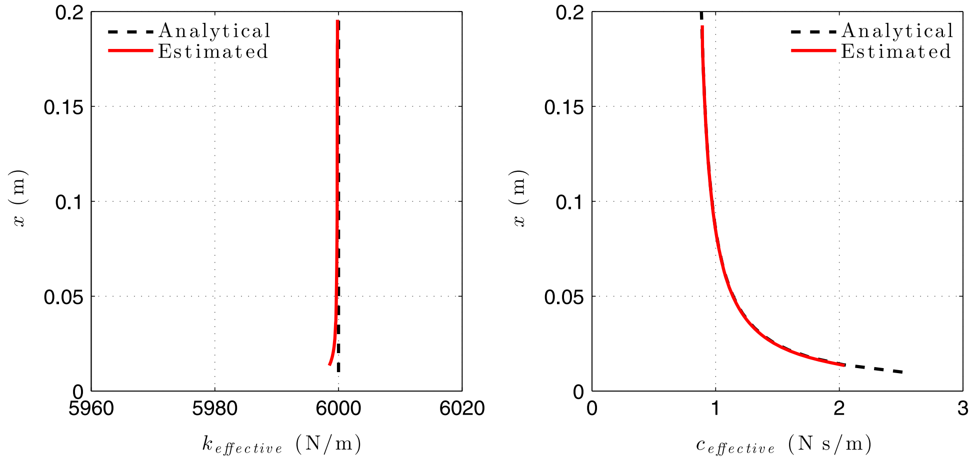

Fig. 4. Effective stiffness and damping estimated from the backbone curve of the SDOF with dry friction.

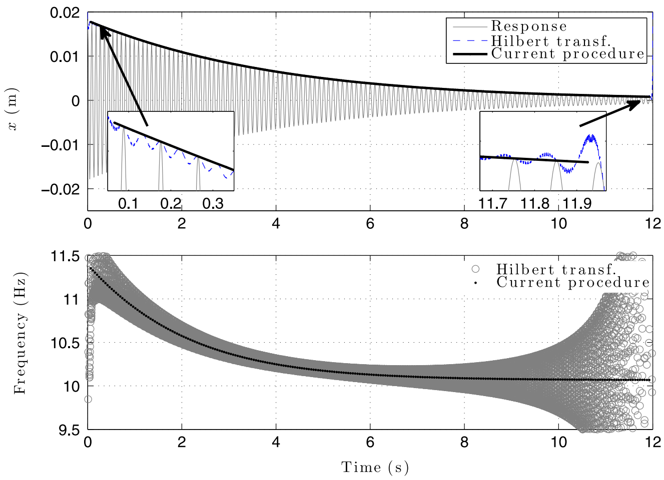

Fig. 5. Approximation of decaying envelope and instantaneous frequency using Hilbert transform and the procedure presented here.

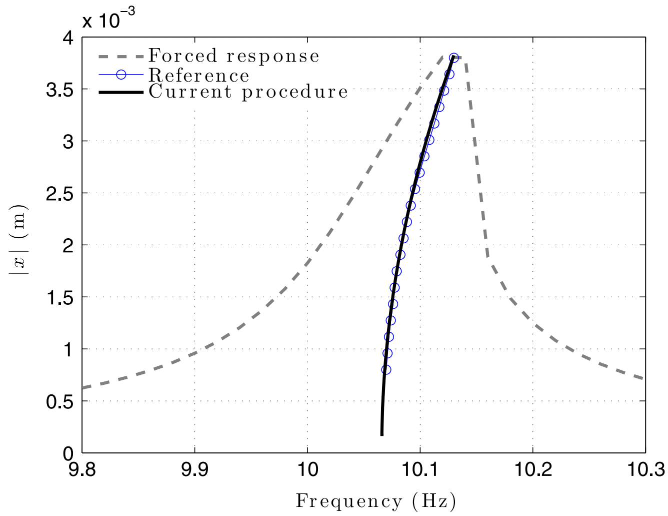

Fig. 6. Comparison between the backbone curves approximated using the procedure presented here and in [17]. A low vibration level is considered.

estimated using the raw amplitude envelope computed using the formulas proposed in [8]. The results show a comparable and satisfactory performance of both procedures in terms of the estimation of the decay envelope. Only minor differences can be observed being more pronounced around the initial and final ends of the decay records and for cases where the nonlinear force affects the structural response more significantly (see the zoomed plots in Fig. 5). These small oscillations in the envelope cause larger dispersion in terms of the instantaneous frequency when estimated using the Hilbert transform approach. We note that this consequence tends to be more pronounced in the presence of noise.

Another approach for extracting backbone curves is presented by Carrella and Ewins [17]. This method relies on the availability of a complete stepped sine sweep response of the system around the resonance frequency of interest. Both sides of the forced response are used to approximate frequency and damping as a function of the response amplitude. Fig. 6 presents results of the estimated backbone curve using the approach in [17] and the one presented here. As before, the case of a SDOF with cubic stiffness is investigated under different levels of external excitation. Results show good match between both approaches when estimating the backbone curves in the case of low vibration levels. However, when the vibration level is stronger, the nonlinearity produces the characteristic jump in the forced response due to the existence of a multiple solution region. As discussed in [17], this discontinuity in the forced response results in giving poor results.

Since the procedure presented here uses a decaying record, it can potentially be applied for any large level of vibration successfully. This offers the possibility of extending the range where a nonlinear system is investigated. It is worth noting that the larger the oscillations, the more the nonlinearities are activated and in turn the more information will be present in the decay response.

4. Experimental example

A simple experimental rig is used to demonstrate the applicability of the procedure and how it copes with real experimental data. Fig. 7 shows the setup of the experiment presented in this work. A base-excited mass was mounted on low-friction linear bearings that slide along two parallel steel shafts. The mass is attached to two grounded pretensioned transversal springs. The springs produce a distinctive nonlinear stiffness that can be adjusted by changing either the static tension in the springs (f_o) or the spring stiffness (k_s).

The dynamics of this system can be approximated by

$$m\ddot{x}+c_d\,\mathrm{sign}(\dot{x})+2x\left(k_s+\frac{f_o-k_s a}{(a^2+x^2)^{1/2}}\right)=0 \tag{11}$$

where x is the displacement of the mass along the shafts; c_d represents the dry friction produced by the linear ball bearings and $a=100$ mm is the distance between the spring supports (see Fig. 7b). The moving mass and spring stiffness were measured to be respectively 2.1 kg and 200 N/m; and the static tension was estimated to be 8.89 N. After taking the first-order expansion of the Harmonic Balance method, it is found that the equivalent stiffness for this system can be approximated by

$$k_{\mathrm{effective}}=2\left(k_s+\frac{f_o-k_s a}{(a^2+x^2/2)^{1/2}}\right) \tag{12}$$

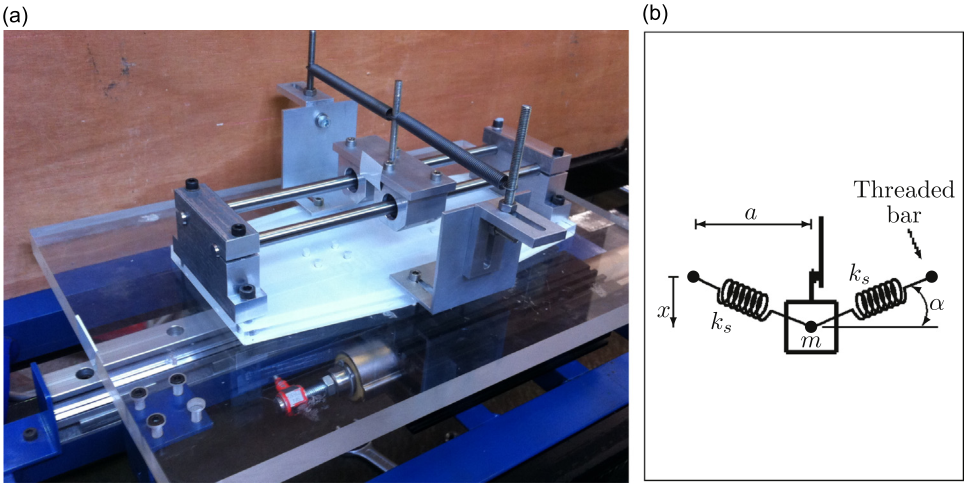

Fig. 7. (a) Experimental rig of a base-excited SDOF system with nonlinear stiffness and friction. (b) Schematic of the SDOF system with nonlinear stiffness.

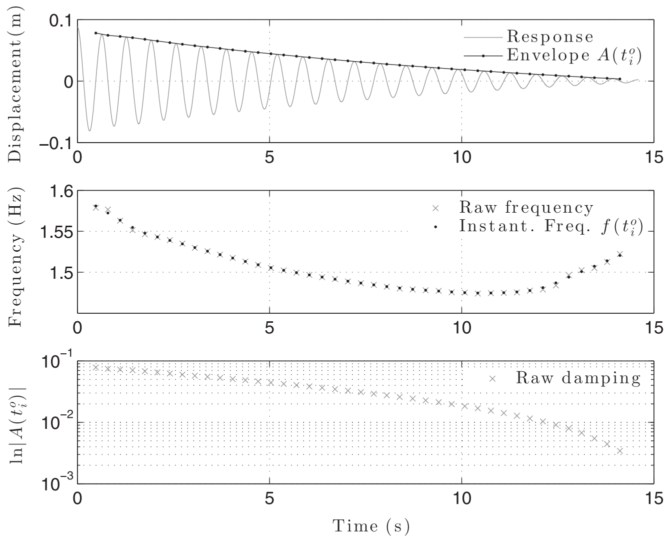

Fig. 8. Estimation of envelope, instantaneous frequency and damping ratio from experimental data.

From three arbitrary large initial conditions, the decaying response was recorded using a DS1104 Dspace board. A PCB 33M07 piezoelectric accelerometer was used to measure the mass response. The sampling rate considered was 512 Hz. The acceleration signals were numerically integrated twice to obtain the system displacements. An offline zero-phase high-pass digital filter was used to operate a baseline compensation (function `filtfilt` in Matlab). This displacement measurement was verified using a laser vibrometer. The amplitude envelope, instantaneous frequency and damping ratio were estimated using the procedure described above. The results for the data recorded in the first test are shown in Fig. 8 and the skeleton curves extracted from all three tests are presented in Fig. 9. The results plotted in the right-hand panel accurately capture the characteristic shape of damping ratio due to dry friction (see, e.g., Fig. 4). Nonetheless, some dispersion can be seen in the estimated instantaneous frequencies of the three tests at the range of displacements less than about 10 mm. As discussed before, the approximation for the instantaneous frequency becomes inaccurate at small amplitude oscillations due to the assumption that damping does not influence the frequency not being fulfilled due to the presence of dry friction (see case 3 in Section 3). Fig. 10 presents a comparison between the effective stiffness estimated from the backbone curve and the theoretical approximation based on the model in Eq. (12). A satisfactory agreement can be observed in the results for large and medium range of displacements. This confirms a successful estimation of the backbone curve in that domain. Note that some discrepancies at large mass displacements (≥ 65 mm) can be seen. This phenomenon is due to the fact that the hooks at the end of the springs start to slide around the threaded anchoring bars for large angles α in Fig. 7b. This physical effect is not modelled in Eq. (11) but is observable in the backbone curves measured. We also note

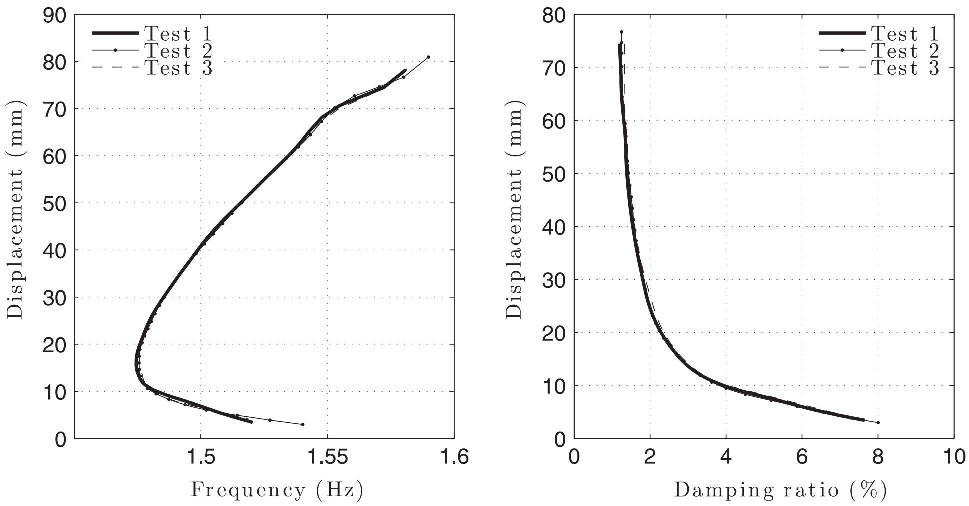

Fig. 9. Skeleton curves estimated from experimental data.

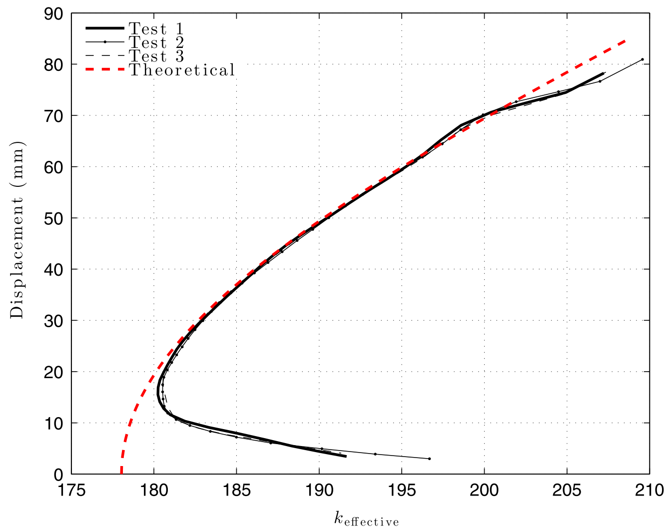

Fig. 10. Effective stiffness estimated from the backbone curve of the experimental SDOF with friction and nonlinear stiffness.

that c_d can be estimated by curve-fitting the damping data in Fig. 9 for the approximate expression of dry friction damping presented in Table 2, this leads to the fit $c_d = 0.08$ N.

5. Application to MDOF systems

A nonlinear MDOF system is now examined. The aim is to show how the procedure introduced above can be extended to estimate backbone curves of multi-degree of freedom systems. This can be accomplished by applying the proposed procedure either to responses of individual masses in physical coordinates or to individual modal coordinates after projecting the system responses into a linear modal space. The example model studied is taken from [18] and consists of two masses connected to ground and between themselves with a linear spring. A cubic spring is located between the first mass and ground and has a positive coefficient of 0.5 N/m^3 to produce a hardening effect on the system response. The underlying linear system is symmetric with masses of 1.0 kg and linear stiffnesses corresponding to 1.0 N/m. The linearised natural frequencies are 1 and $\sqrt{3}$ rad/s and the mode shapes are $[1,1]^{\mathrm{T}}$ and $[-1,1]^{\mathrm{T}}$. The system dynamics are represented by the set of equations

$$\begin{aligned} \ddot{x}_1 + 0.03\dot{x}_1 + (2x_1 - x_2) + 0.5x_1^3 &= p_1 \\ \ddot{x}_2 + 0.01\dot{x}_2 + (2x_2 - x_1) &= p_2 \end{aligned} \tag{13}$$

where x_1 and x_2 are the displacements of masses 1 and 2 respectively, and p_1 and p_2 are the external loads applied to the corresponding masses.

As mentioned in Section 2.1, a suitable force pattern is needed to excite the structure at one specific mode. It is essential to achieve the steady-state response from which the decay record can be properly originated. This ensures that the frequency content in the response signal will allow for a correct identification of the skeleton curves. After applying the Normal-Force Mode Appropriation method [15], the Multivariate Mode Indicator Functions (MMIF) showed that only one input (either p_1 or p_2) is required to isolate each vibration mode and to obtain the desired resonance condition of the system. Thus without loss of generality, $[p_1, p_2] = [p_{1_0} \sin \omega t, 0]$ is used as the force pattern. This force vector is applied to the system close to the first linear natural resonance frequency and tuned in both amplitude and frequency until the amplitude of the response is large enough to excite the nonlinearity and the response is approximately resonant. When the system response reached a steady-state condition, the force is removed and the decay response recorded.

Fig. 11 shows the resulting decay records measured from the resonance condition for the first characteristic frequency. The amplitude envelope, instantaneous frequency and damping are estimated for individual displacement records in physical space, following the procedure proposed in this paper. The process was then repeated for the second characteristic frequency and the resulting decay responses recorded and analysed. Finally, the identified amplitude envelope and instantaneous frequency were combined to produce the backbone curves, these are plotted in solid black line in Fig. 12. They are superimposed onto several synthetic stepped-sine sweep responses for different levels of excitation $\left(p_{1_0} = \{0.005, 0.01, 0.02, 0.05, 0.1, 0.2\}\ \mathrm{N}\right)$. Both the sweep up and down responses around the two natural frequencies of the system are included in the figure. These results reveal an excellent match between the estimated backbone curve and the trajectory that connects all the maxima of the force responses of the nonlinear system. This strong agreement can be seen in the displacements of both masses and for the two resonance frequencies, indicating a successful and accurate estimation of the backbone curves.

It could be argued that the backbone curves can be derived approximately from a complete set of stepped-sine sweep responses (see for instance [17]), provided that shakers have sufficient control to ensure that the forces amplitude remains constant despite the coupling with the nonlinear system. Nonetheless, it is worth noting that each point of the forced

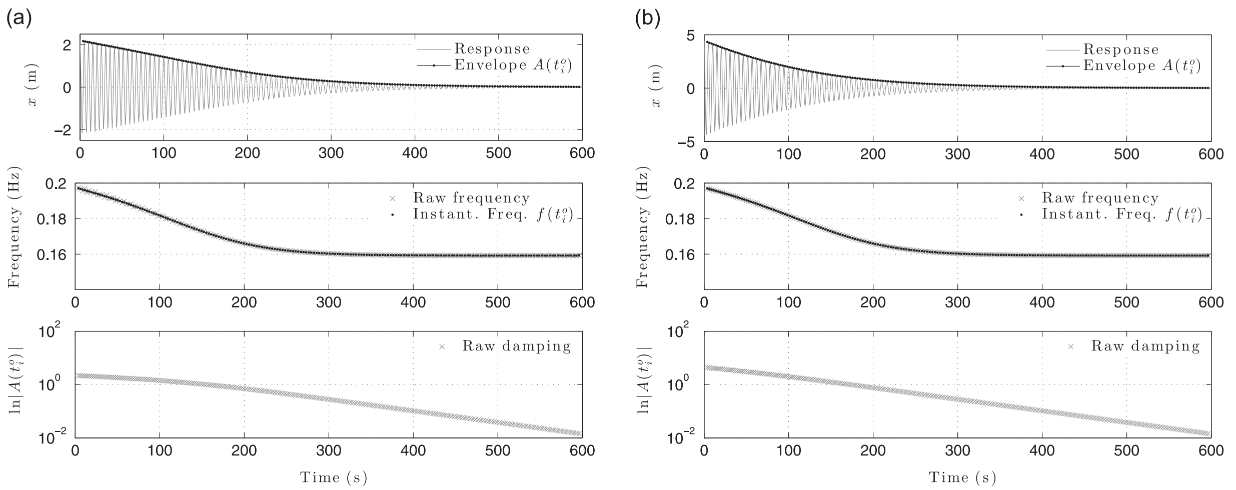

Fig. 11. Estimation of envelope, instantaneous frequency and damping for the system in (13) from the decay records originated around the first resonance frequency. (a) Displacement of mass 1, x_1. (b) Displacement of mass 2, x_2.

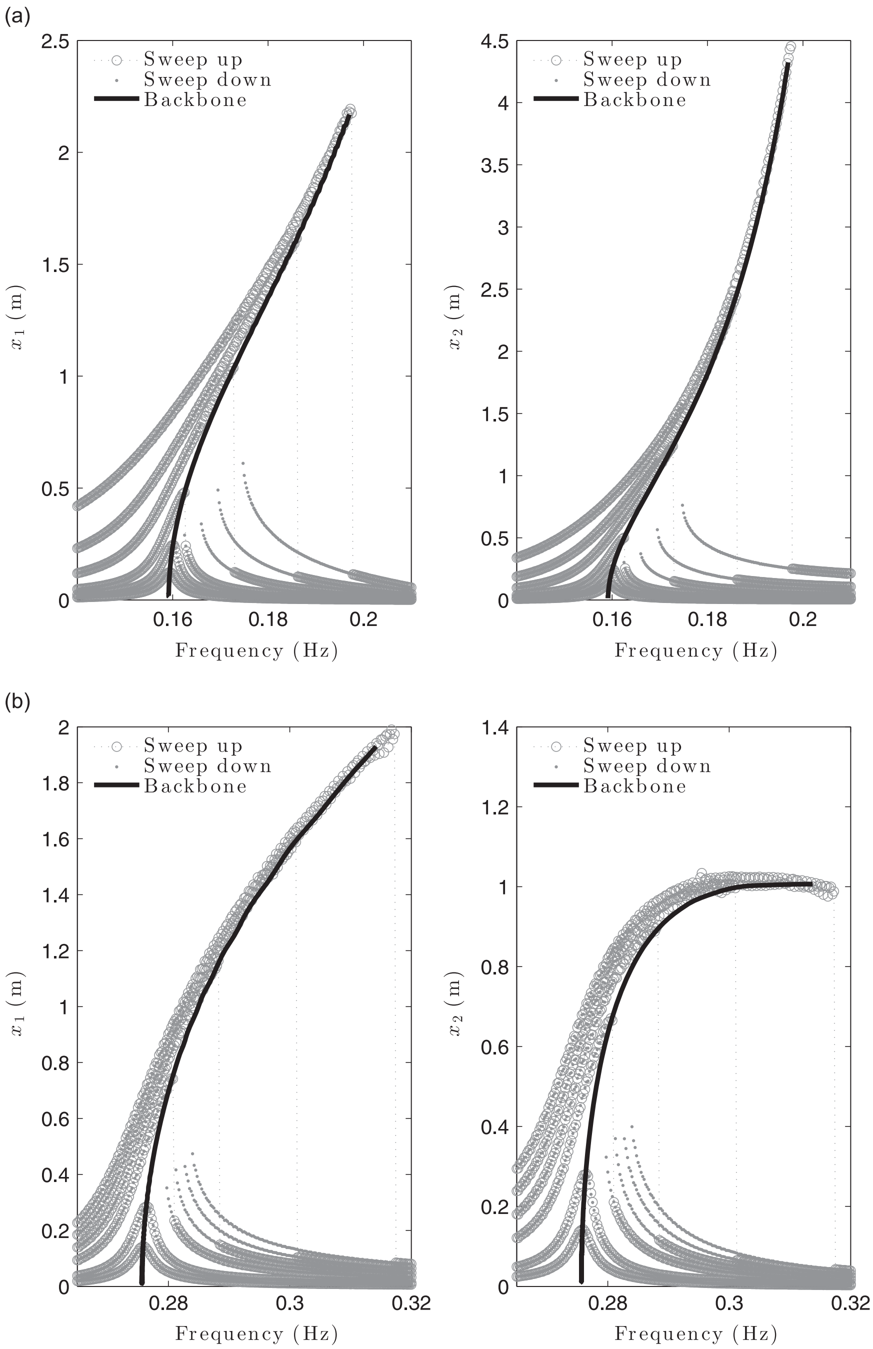

Fig. 12. Backbone curves estimated using the procedure proposed in this paper. (a) For the first resonance frequency. (b) For the second resonance frequency.

response corresponds to the steady state of the system when excited at a specific frequency and forcing level. It represents a large experimental effort to obtain a complete set of frequencies' responses, in particular when testing lightly damped systems at high forcing levels and around the resonance peaks. Conversely, the proposed method offers the possibility of extracting the backbone curves from single resonance decay responses for each resonance frequency.

One can use the matrix of mode shapes Φ of the underlying linear system in (13) to transform the system responses into their representation in modal space [1]. Following this, individual responses in modal coordinates can be evaluated in accordance with the procedure described in Section 2. In this case, the set of estimated backbone curves is a particular representation in the modal space defined by the linear transformation Φ. Fig. 13 shows the backbone curves estimated in modal coordinates for both resonance frequencies. The results around the first resonance frequency indicate that most of the responses (and so the information of the nonlinearity) are included in the backbone curve estimated in terms of the first modal coordinate q_1. However,

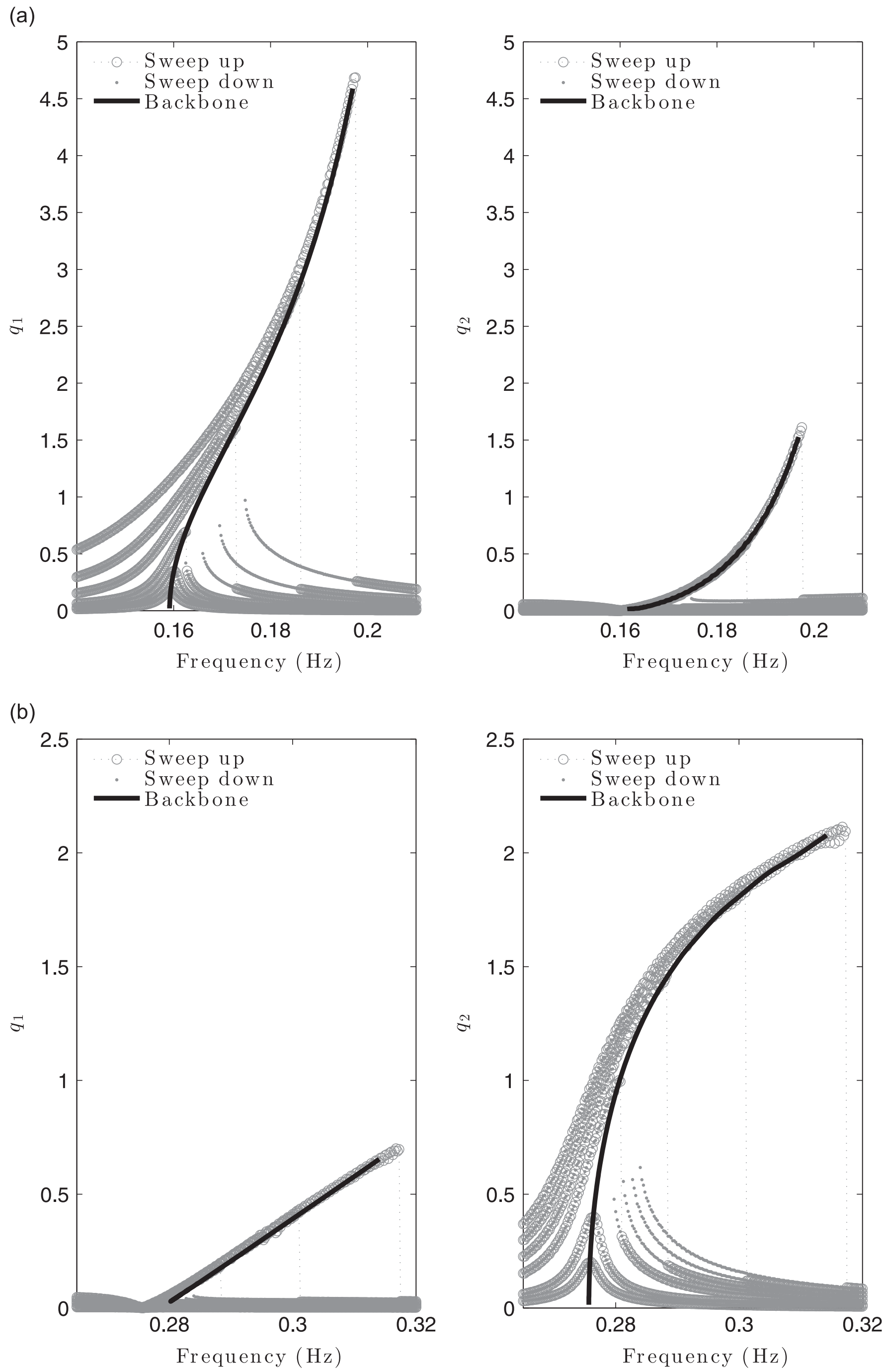

Fig. 13. Backbone curves in modal coordinates q_1 and q_2. (a) For the first resonance frequency. (b) For the second resonance frequency.

it can be seen that when the response becomes larger, the influence of the nonlinearity is more significant with the backbone curve of the second modal coordinate q_2 starting to increase. This nonlinear effect is due to the interaction between the linear modes, in fact the backbone curve relates directly to the nonlinear normal modes of the system [18]. A similar effect is seen in Fig. 13b with reference to the responses around the second resonance frequency.

To further validate the estimated backbone curves, precise numerical solutions for the backbone curves are calculated using the AUTO[1] [19], a numerical continuation and bifurcation analysis software package. Fig. 14 compares the backbone

[1] http://indy.cs.concordia.ca/auto

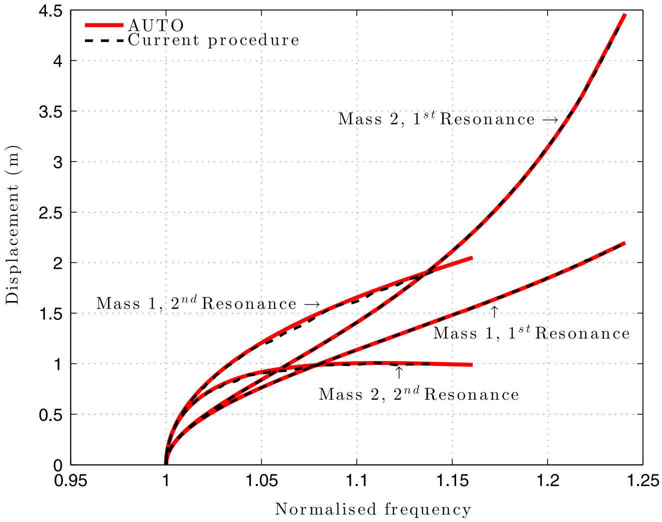

Fig. 14. Comparison of the estimated backbone curves of the system in Eq. (13) with respect to the solutions using numerical continuation (AUTO). Amplitudes are in physical coordinates and frequencies are normalised with respect to the natural linear frequencies.

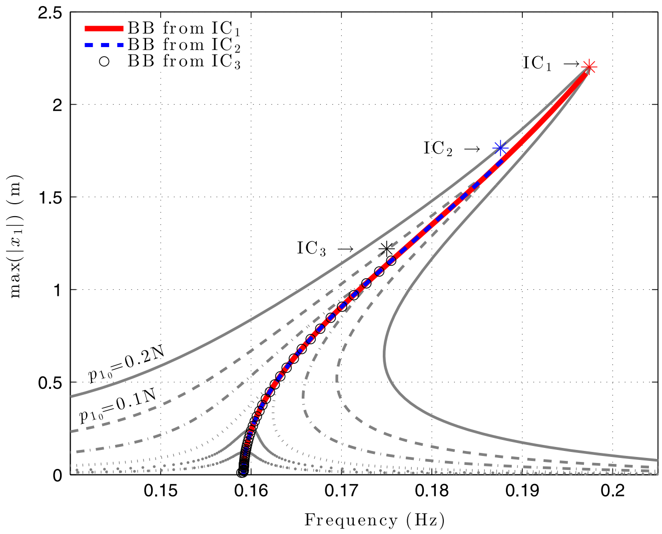

Fig. 15. Forced responses of mass 1 of the system in (13) for different levels of harmonic excitation p_{1_0} and backbone (BB) curves computed from decay records generated from different initial conditions (IC). (For interpretation of the references to color in this figure, the reader is referred to the web version of this paper.)

curves of the system in Eq. (13) using the procedure presented in this paper with those results obtained using numerical continuation. Note that the maximum error in the displacement prediction is 1 per cent and occurs for a medium amplitude of the first mass in the second resonant response.

It is worth noting that more elaborated cases of nonlinear coupling could be studied using techniques based on backbone curves [20,21]. However, this is still a open research topic that needs to be further explored in order to identify the limitations of the proposed method in estimating backbone curves when more complex interactions occur.

5.1. Sensitivity to initial conditions

So far, arbitrary resonant responses, and so initial conditions, have been selected to generate the structural responses examined. This section discusses how the use of different resonant responses when generating the decay records could affect the estimation of backbone curves. This is relevant as for experimental tests the system is first excited in a resonance condition before being released.

Fig. 15 presents the forced responses of the MDOF system in Eq. (13) for a range of different levels of sinusoidal excitation. Three different resonant conditions have been used to generate the decay response records and estimate the corresponding backbone curves. The first resonant condition (IC_1) corresponds to the forcing level $p_{1_0} = 0.2$ N and the frequency at which the maximum response is produced (this condition corresponds to the fold bifurcation point). The second resonant condition (IC_2) is on the same branch of forcing level $p_{1_0} = 0.2$ N but at a frequency well below the fold bifurcation point. The IC_3 is chosen for the forcing level $p_{1_0} = 0.1$ N and an arbitrary frequency lower than the corresponding fold bifurcation point. The backbone curve estimated using the decay record generated from IC_1 is plotted using a thick red line, the one estimated from IC_2 is plotted using a blue dashed line whilst the curve estimated from IC_3 is plotted using black circles.

The three backbone curves follow the same path independent of the initial condition used to generate the decay records. Several other resonance conditions were investigated obtaining the same result; they are not plotted here for simplicity in the figure. The results confirm that the initial condition used to generate the decay records does not affect the resulting estimation of the backbone curves as long as it lies on a resonant response of the system and is large enough to activate the nonlinearity.

6. Conclusions

The prediction of the performance of nonlinear structural systems is an increasingly important research topic. Among other analysing tools, backbone curves stand out as they offer the advantage of a better understanding of their dynamical behaviour. In this paper, a procedure has been presented to be able to extract backbone curves of nonlinear system from decay responses. This approach is well suited to investigate structures that are primarily linear, but contain nonlinear elements which become significant at larger excitation levels. Such characteristics are typical of many industrial scale flexible structures to which geometric nonlinearities occur.

Results obtained from simulated and real experiments demonstrated that the proposed procedure is capable of achieving an accurate estimation of the backbone curves and damping ratio skeletons. The case of dry friction was discussed to show that the approximation of instantaneous frequency can become inaccurate if the assumption of damping having low influence on frequency is not nearly fulfilled. Results suggest that damping ratios lower than 5 per cent does not significantly affect the estimation of the instantaneous frequency of the nonlinear system. However, more investigation is needed in order to identify the amount of damping above which the method presented here loses accuracy.

It was also shown that the initial condition used to generate the decay records do not affect notably the resulting estimation of the backbone curve as long as it lies on a steady-state trajectory of the system. It was shown how the proposed approach can be successfully applied to a MDOF system. Further work is required to establish a strategy to extract the nonlinear structural parameters from a set of backbone curves. This will allow for full system identification. Further efforts will be addressed particularly to identification in terms of the modal coordinates.

Further exploration is being done to identify the limitations of the presented methodology in case of more complex nonlinear interaction in MDOF systems where the estimation of backbone curves may become challenging or even impossible due, for instance, to two interacting closer modes.

Acknowledgement

The present work was funded by the Engineering and Physical Sciences Research Council (EPSRC) in the UK as part of the Engineering Nonlinearity Programme Grant EP/K003836/1. Prof. S.A. Neild is supported by the EPSRC Fellowship EP/K005375/1 and Prof. J. E. Cooper is supported by the Royal Academy of Engineering in the UK through the RAEng Airbus Sir George White Chair in Aerospace Engineering. This financial support is gratefully acknowledged.

References

[1] D. Ewins, *Modal Testing: Theory*, *Practice and Application*, *Engineering Dynamics Series*, 2nd edition, RSP LTD, Baldock, Hertfordshire, UK, 2000.
[2] K. Worden, G. Tomlinson, *Nonlinearity in Structural Dynamics: Detection, Identification and Modelling*, IOP Publishing Ltd, Bristol, Philadelphia, 2001.
[3] A. Carri, D. Ewins, A systematic approach to modal testing of nonlinear structures, R. Allemang, J. De Clerck, C. Niezrecki, A. Wicks (Eds.), *Topics in Modal Analysis Conference Proceedings of the Society for Experimental Mechanics Series*, Vol. 7, Springer, New York2014, pp. 273–286, http://dx.doi.org/10.1007/978-1-4614-6585-0_25.
[4] D.J. Wagg, S.A. Neild, *Nonlinear Vibration with Control, Solid Mechanics and Its Applications*, Vol. 170, Springer-Verlag, Dordrecht, The Netherlands, 2010.
[5] J.M. Londono, S.A. Neild, J.E. Cooper, Systems with bilinear stiffness: *Extraction of backbone curves and identification*, G. Kerschen (Ed.), *Nonlinear Dynamics, Conference Proceedings of the Society for Experimental Mechanics Series*, Vol. 1, Springer International Publishing, Switzerland, 2015. http://dx.doi.org/10.1007/978-3-319-15221-9_27.
[6] A. Cammarano, P. Green, T. Hill, S. Neild, Nonlinear system identification through backbone curves and bayesian inference, G. Kerschen (Ed.), *Nonlinear Dynamics, Conference Proceedings of the Society for Experimental Mechanics Series*, Vol. 1, Springer International Publishing, Switzerland, 2015.
[7] M. Feldman, Non-linear system vibration analysis using Hilbert transform–I. Free vibration analysis method 'Freevib', *Mechanical Systems and Signal Processing* 8 (2) (1994) 119–127, http://dx.doi.org/10.1006/mssp.1994.1011.
[8] M. Feldman, Identification of weakly nonlinearities in multiple coupled oscillators, *Journal of Sound and Vibration* 303 (2) (2007) 357–370, http://dx.doi.org/10.1016/j.jsv.2007.01.028.
[9] W. Staszewski, Identification of damping in MDOF systems using time-scale decomposition, *Journal of Sound and Vibration* 203 (2) (1997) 283–305, http://dx.doi.org/10.1006/jsvi.1996.0864.
[10] W. Staszewski, Identification of non-linear systems using multi-scale ridges and skeletons of the wavelet transform, *Journal of Sound and Vibration* 214 (4) (1998) 639–658, http://dx.doi.org/10.1006/jsvi.1998.1616.
[11] S. Naylor, M.F. Platten, J.R. Wright, J.E. Cooper, Identification of multi-degree of freedom systems with nonproportional damping using the resonant decay method, *Journal of Vibration and Acoustics* 126 (2) (2004) 298–306, http://dx.doi.org/10.1115/1.1687395.
[12] M.F. Platten, J.R. Wright, K. Worden, G. Dimitriadis, J.E. Cooper, Non-linear identification in modal space using a genetic algorithm approach for model selection, *International Journal of Applied Mathematics and Mechanics* 3 (1) (2007) 72–89.

[13] M.F. Platten, J.R. Wright, J.E. Cooper, G. Dimitriadis, Identification of a nonlinear wing structure using an extended modal model, *Journal of Aircraft* 46 (5) (2009) 1614–1626, http://dx.doi.org/10.2514/1.42024.

[14] G. Charmbalis, J.M. Londono, J.E. Cooper, *Vibration Testing of Aeroelastic Structures Containing Geometric Stiffness Nonlinearities*, American Institute of Aeronautics and Astronautics, Boston, 2013 http://dx.doi.org/10.2514/6.2013-1561.

[15] J.R. Wright, J.E. Cooper, M.J. Desforges, Normal-mode force appropriation—theory and application, *Mechanical Systems and Signal Processing* 13 (2) (1999) 217–240, http://dx.doi.org/10.1006/mssp.1998.1214.

[16] S.A. Neild, P.D. McFadden, M.S. Williams, A review of time–frequency methods for structural vibration analysis, *Engineering Structures* 25 (6) (2003) 713–728, http://dx.doi.org/10.1016/S0141-0296(02)00194-3.

[17] A. Carrella, D. Ewins, Identifying and quantifying structural nonlinearities in engineering applications from measured frequency response functions, *Mechanical Systems and Signal Processing* 25 (3) (2011) 1011–1027, http://dx.doi.org/10.1016/j.ymssp.2010.09.011.

[18] M. Peeters, G. Kerschen, J. Golinval, Modal testing of nonlinear vibrating structures based on nonlinear normal modes: *experimental demonstration*, *Mechanical Systems and Signal Processing* 25 (4) (2011) 1227–1247, http://dx.doi.org/10.1016/j.ymssp.2010.11.006.

[19] A.R. Champneys, Y.A. Kuznetsov, B. Sandstede, A numerical toolbox for homoclinic bifurcation analysis, *International Journal of Bifurcation and Chaos* 6 (5) (1996) 867–887, http://dx.doi.org/10.1142/S0218127496000485.

[20] T.L. Hill, A. Cammarano, S.A. Neild, D.J. Wagg, Out-of-unison resonance in weakly nonlinear coupled oscillators, *Proceedings of the Royal Society of London A: Mathematical Physical and Engineering Sciences* 471 (2173) (2015). http://dx.doi.org/10.1098/rspa.2014.0659.

[21] R. Lewandowski, On beams membranes and plates vibration backbone curves in cases of internal resonance, *Meccanica* 31 (3) (1996) 323–346, http://dx.doi.org/10.1007/BF00426994.